TOPOGRAPHY AND INFLATION FEATURES OF THE 1859 MAUNA LOA LAVA FLOW, HAWAI'I: APPLICATIONS TO INFLATED FLOWS ON MARS. W. B. Garry[1], J. R. Zimbelman[1], J. E. Bleacher[2], L. S. Crumpler[3]. [1]Center for Earth and Planetary Studies, Smithsonian Institution, National Air and Space Museum MRC 315, Washington, DC, 20013, garryw@si.edu, [2]Planetary Geodynamics Laboratory, Code 698, NASA Goddard Space Flight Center, Greenbelt, MD, 20771, [3]New Mexico Museum of Natural History and Science, Albuquerque, NM, 87104.

Introduction: The final flow morphology of effusive lava flows can be used to interpret emplacement parameters and rheologic properties [e.g.1-3], but there is a concern that these results may not be representative of a flow's initial emplacement parameters [4]. Observations of active lava flows and detailed studies of emplaced flow features on the centimeter to meter scale reveal the subtle, complex processes that occur to form the final morphology on a kilometer scale [e.g. 5-10]. It is important to know how smaller-scale (cm to m) topography and flow features (surface textures, layers, squeeze ups) relate to larger-scale (m to km) features (terraced margins, tumuli, platforms, levees) observable in remote sensing images for making plausible interpretations of lava flows on other planetary bodies based solely on morphologic observations [e.g. 3,11]. Here, we will present our field documentation of the topography and surface textures of the inflated, distal end of the pāhoehoe portion of the 1859 Mauna Loa lava flow, Hawai'i (hereafter: 1859 Flow) (Fig. 1) in an effort to identify specific characteristics of low-effusion-rate flows that can potentially be observed on lava flows with remote sensing data, both on Earth and on planetary surfaces.

Data Collection: Preliminary field observations were made in August 2008. We used a LIDAR (Light Detection And Ranging) system (Model: Optech ILRIS-3D) to collect representative topographic data along the margin of the 'a'ā flow and the inflated surface of the pāhoehoe (Fig. 2c). In February 2009, we will complete a systematic topographic survey across the inflated pāhoehoe surface using a Trimble R8 Differential Global Positioning System (DGPS). The DGPS we will use has a vertical accuracy of 2 to 4 cm and a horizontal accuracy of 1 to 2 cm. Detailed field observations of flow textures and features on the centimeter to meter scale will also be made.

1859 Mauna Loa Flow, Hawai'i. The 1859 Flow is the longest historic lava flow (51 km) in Hawai'i; it is a prime example of a 'paired' lava flow where both 'a'ā (accumulations of spiny clinkers) and pāhoehoe (smooth to ropy glassy surface) comprise distinct portions of the final flow [12]. The eruption started January 23 from a linear vent high on the north side of Mauna Loa, where lava fountains fed an 'a'ā flow through February 7, followed by effusion confined to a tube system that supplied a pāhoehoe flow field until the eruption ended in late November [12,13]. Walker [7] described many distinctive landforms on Hawaiian lavas that are the result of injection of lava under a cooled surface crust, including tumuli, lava rises, and lava-rise pits; he also pointed out that numerous lava-rise pits on the distal portion of the 1859 flow have overhanging rims. We intend to document the shapes and dimensions of the inflation features on the 1859 lava flow.

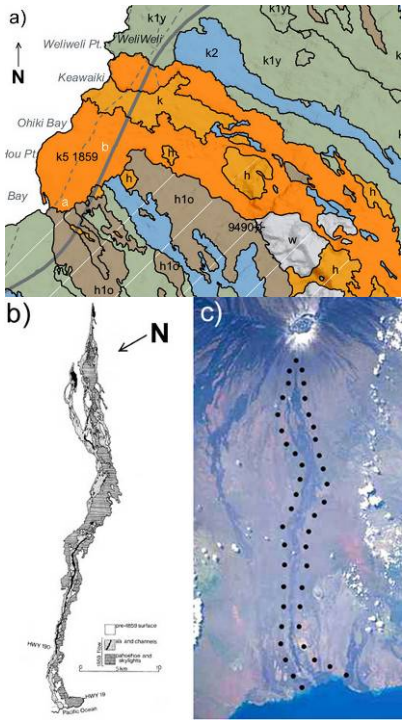

Figure 1. a) Geologic map of the distal end of 1859 flow (orange k5 unit), from [14]. White letters show locations of Figs 2a&b. b) Map of 1859 flow, from Fig. 4 of [12]. c) 1859 flow, outlined by dots. NASA, ISS004-729-67, 2000.

Upcoming Field Work. Our work will focus on the distal portion of the inflated pāhoehoe component of the 1859 Flow. The general distribution of both 'a'ā and pāhoehoe for this flow were mapped from aerial photographs [12] (Fig. 1b), and photographs taken by astronauts on the International Space Station (ISS) provide excellent context for the entire flow (Fig. 1c). Lava-rise pits on the distal portion of the 1859 flow are distinguishable from collapse pits by the way the rim forms a distinct overhang during the inflation process [7]. Google Earth reveals both lava rise platforms and

lava-rise pits. Specific inflation features to be investigated include lava rises (Fig. 2a), lava-rise pits (Fig. 2a and b), tumulus ridges (Fig. 2b), and terraced flow margins. Lava-rise pits represent regions left depressed by inflation of the surrounding lava [e.g. 15, 16]. For the lava rises, we will use DGPS to obtain precise topographic profiles across the rise platform both parallel and perpendicular to the regional slope. For lava-rise pits, we will measure profiles across the pit and the slopes of the interior walls in the pit. Tumuli (broad swells in the lava surface, often topped by a large fracture [17, 18] (Fig. 2c); are abundant on inflated flows, with a classic study of these features on the McCartys lava flow in New Mexico [19]. For tumuli, we will measure profiles both across and along the long axis of the feature. These measurements should provide precise quantitative attributes for diagnostic identification of inflation features in remote sensing data.

Application of Field Results to Remotely Sensed Data and Mars. Use of a combination of distinct textural attributes along with the horizontal and vertical scales over which these features are expressed should provide the basis to interpret the inflation history expressed within each flow field. Field mapping will aid in identifying discreet lobes within the overall flow field, something suggested for the Carrizozo flow by early DGPS results [20], but which only recently was documented by DGPS data [21]; similar flow lobes may also become evident within the distal portions of the 1859 as the work progresses. The information compiled in our mapping products will be at a scale that is comparable to the excellent remote sensing data currently available for Mars, so that the textural maps should be directly applicable to the interpretation of the lava flows on Mars [21], and eventually to flows on several other planetary surfaces as well. Here, we intend to synthesize our results in terms of the sensor capabilities and spatial resolution that would be required to observe features that are diagnostic of flow inflation using remote sensing data. Such a synthesis would potentially be applicable both to future remote sensing studies of lava flows on Earth, as well as to lava flows observed on other planetary surfaces.

Acknowledgements: This work is supported by a research grant from the Smithsonian Institution Scholarly Studies Program, and it will compliment a recently approved (but not yet funded) grant from the NASA PG&G program.

References: [1] Hulme G. (1974) *Geophys. J. Int. 39*, 361-383. [2] Fink J.H. and Zimbelman J.R. (1986) *Bull. Volcanol. 48,* 87-96. [3] Garry W.B. et al. (2007) *JGR, 112,* E08007, doi:10.1029/2006JE002803. [4] Harris J.L. et al. (2008) *Bull. Volcanol.,* doi: 10.1007/s00445-008-0238-6. [5] Greeley R. (1971) *Modern Geology, 2,* 207-223. [6] Lipman P.W. and Banks N.G. (1987) *USGS Prof. Pap. 1350,* 1527-1567. [7] Walker G.P.L. (1991) *Bull. Volcanol., 53,* 546-558. [8] Hon K. et al. (1994) *GSA Bull., 106,* 351-370. [9] Anderson S.W. et al. (1999) *EPSL, 168,* 7-18. [10] Crown D.A. and Baloga S.M. (1999) *Bull. Volcanol., 61,* 288-305. [11] Baloga S.M. et al. (2003) JGR, 108, E7, 5066, doi:10.1029/2002JE001981. [12] Rowland S.K. and Walker G.P.L. (1990) *Bull. Volcanol., 52,* 615-628. [13] Haskell R.C. (1859) *Am. J. Sci., 78,* 66-71. [14] Wolfe E.W. and Morris J. (1986) *Geologic Map of Hawaii*, I-2524-A. [15] Self S. et al. (1997) *in Large Igneous Provinces, AGU Monograph 100,* 381-410. [16] Keszthelyi L. and McEwen A. (2007) *in The Geology of Mars,* Cambridge Univ. Press, 126-150. [17] Francis P. (1993) *Volcanoes: A planetary perspective,* Clarendon Press, 443 p. [18] Glaze L.S. (2005) *JGR, 110,* B08202, doi: 10.1029/2004JB003564. [19] Nichols R.L. (1946) *GSA Bull., 57,* 1049-1086. [20] Zimbelman J.R. and Johnston A.K. (2001) *in Volcanology in New Mexico, New Mexico Mus. Nat. Hist. and Sci., Bulletin 18,* 131-136. [21] Garry W.B. (2008) *LPSC 39*, Abstract #1734.

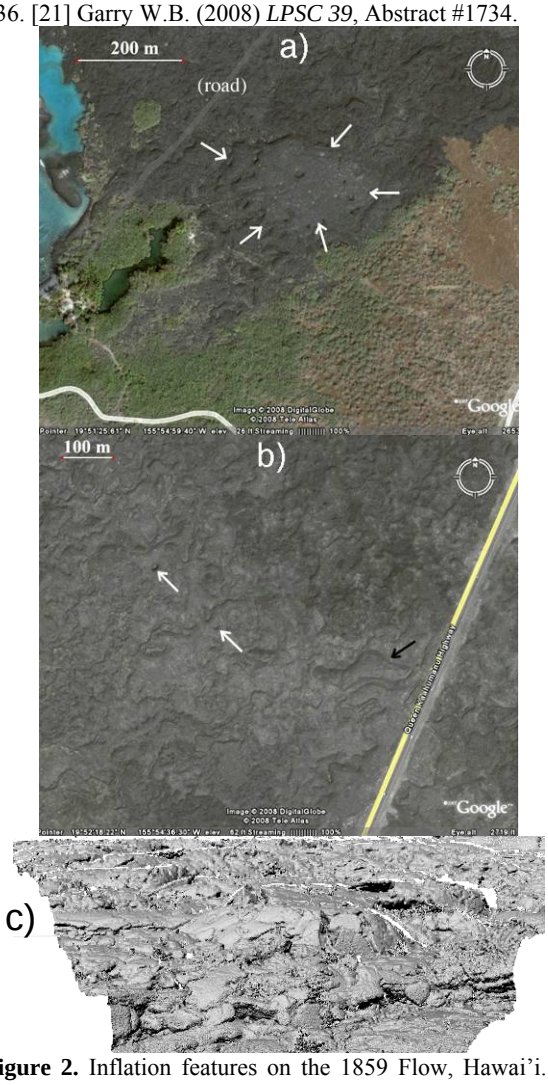

Figure 2. Inflation features on the 1859 Flow, Hawai'i. a) Arrows indicate a lava rise platform with a lava-rise pit near its center, surrounded by other inflation landforms. b) White arrows indicate lava-rise pits; black arrow indicates a tumulus ridge (Google Earth). c) LIDAR topography of inflated pāhoehoe surface. Tumulus located in central part of image.